





respectively.<sup>13,47,55</sup> There was no obvious difference in the position of Fe 2p of these samples, but CeNiFe-MOF was superior in the content of Fe<sup>3+</sup> to pristine NiFe-MOF (Fig. S3†), indicating that the chemical state of Fe has also been regulated after doping with Ce.<sup>34,45,56</sup> The above XPS results clearly revealed that the electronic properties of Ni and Fe could be effectively modulated by the introduction of Ce into NiFe-MOF, which is expected to optimize the electrochemical performance of the as-prepared CeNiFe-MOF.

The electrochemical measurements were first conducted in 1.0 M KOH solution by using a typical three-electrode cell. It is found that the CeNiFe-MOF with the Ce(NO<sub>3</sub>)<sub>3</sub>·6H<sub>2</sub>O addition amount of 0.05 mmol showed the best electrocatalytic performance (Fig. S4 and S5†). The content of Ce in this optimal CeNiFe-MOF composite was determined to be 0.59 wt% by

inductively coupled plasma mass spectrometry (ICP-MS). Compared to pristine NiFe-MOF, the HER overpotential of CeNiFe-MOF was more close to that of commercial Pt/C (Fig. 3a and S6†). Specifically, CeNiFe-MOF exhibited a relatively lower value of 113 mV at 10 mA cm<sup>-2</sup> than NiFe-MOF (151 mV), suggesting that the introduction of Ce is beneficial for the improvement of HER activity. The Tafel slope of 59.4 mV dec<sup>-1</sup> was observed for CeNiFe-MOF (Fig. 3b), which was much lower than that of pristine NiFe-MOF (71.3 mV dec<sup>-1</sup>). This smaller Tafel slope is indicative of the superior reaction rates of CeNiFe-MOF for the HER with the Volmer–Heyrovsky mechanism.<sup>3,19,57,58</sup> As exhibited in Fig. 3c, the self-supporting CeNiFe-MOF electrode also delivered favorable OER activity with an overpotential of only 198 mV at 100 mA cm<sup>-2</sup>, which was 50, 96 and 160 mV lower than those of pristine NiFe-MOF (248 mV),

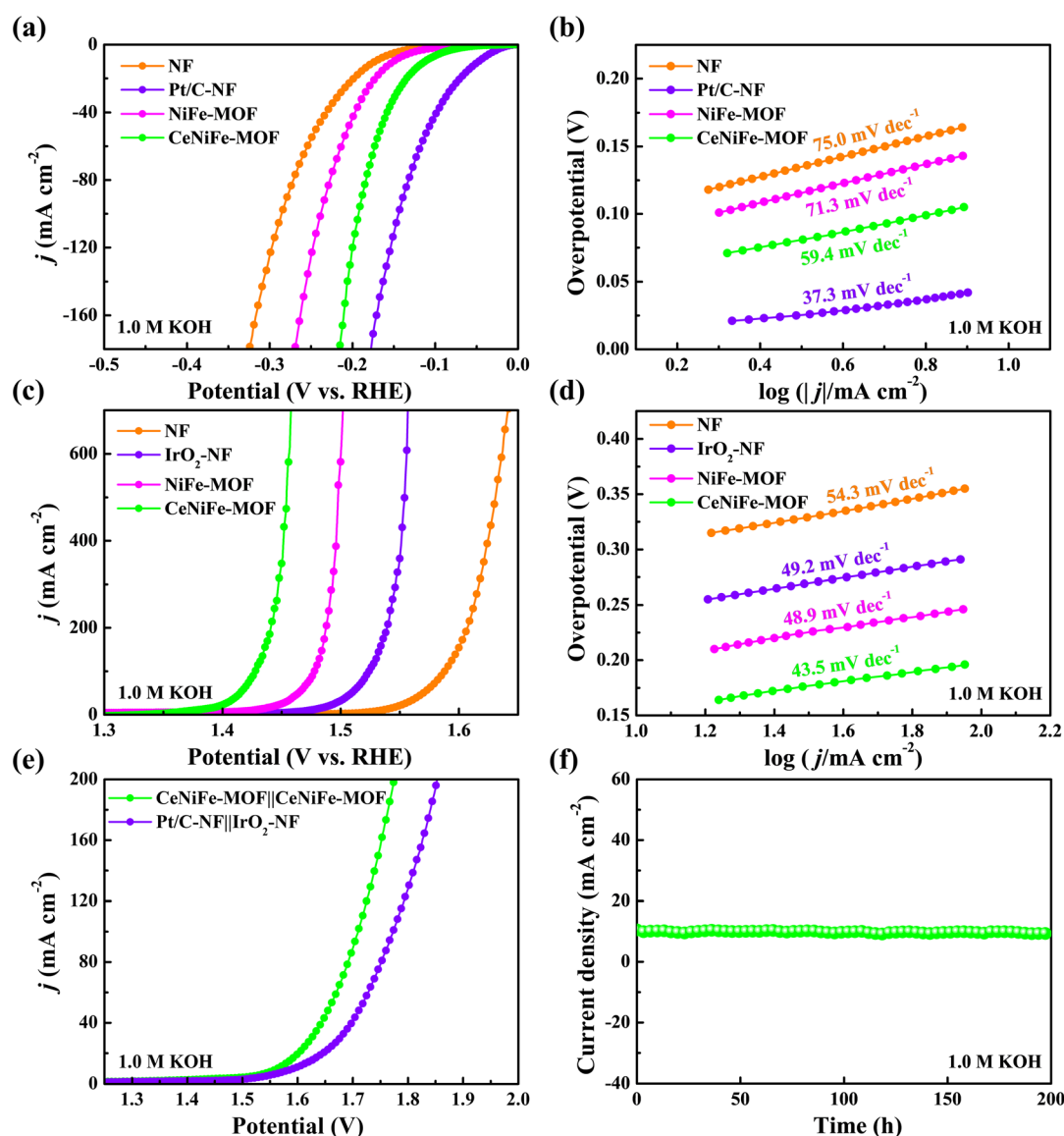


Fig. 3 Electrochemical performance of the samples in 1.0 M KOH. (a) HER polarization curves and (b) the corresponding Tafel slopes. (c) OER polarization curves and (d) the corresponding Tafel slopes. (e) Polarization curves of CeNiFe-MOF||CeNiFe-MOF and Pt/C-NF||IrO<sub>2</sub>-NF for water electrolysis. (f) Chronoamperometry curve of CeNiFe-MOF||CeNiFe-MOF toward overall water splitting.



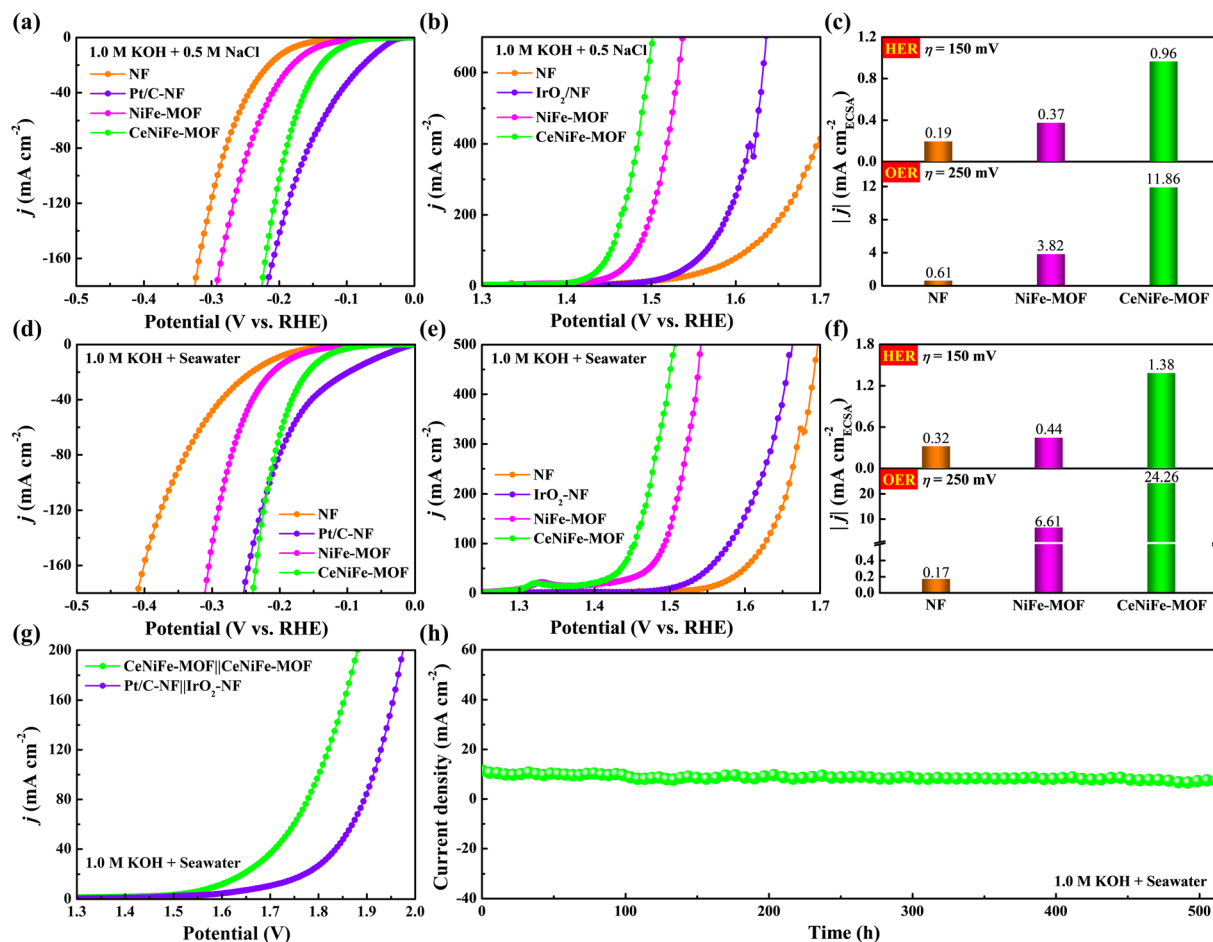


Fig. 4 (a) HER and (b) OER polarization curves of the samples in 1.0 M KOH + 0.5 M NaCl. (c) Comparison of their specific activity in 1.0 M KOH + 0.5 M NaCl. (d) HER and (e) OER polarization curves of the samples in 1.0 M KOH + seawater. (f) Comparison of their specific activity in 1.0 M KOH + seawater. (g) Polarization curves of CeNiFe-MOF||CeNiFe-MOF and Pt/C||IrO<sub>2</sub> for alkaline seawater electrolysis. (h) Chronoamperometry curve of CeNiFe-MOF||CeNiFe-MOF toward overall seawater splitting.

the Fermi level was more than that of pristine NiFe-MOF (Fig. 5a), corresponding to the enhanced conductivity and electron transport capability,<sup>33,66,67</sup> as verified by EIS measurements. Notably, the d-band center of CeNiFe-MOF (−3.09 eV) was much closer to the Fermi level, in comparison to that of NiFe-MOF (−3.47 eV), which indicated the better adsorption of reaction intermediates on active sites.<sup>66–71</sup> The Gibbs free energy of H\* ( $\Delta G_{H^*}$ ) was further calculated to evaluate the HER activity of as-prepared electrocatalysts. As illustrated in Fig. 5b, the Fe in CeNiFe-MOF exhibited the lowest value of  $\Delta G_{H^*}$  (0.1 eV), which was responsible for the accelerated HER kinetics and the improved HER activity.<sup>35</sup> Fig. S34† depicts the free energy for the OER process, where the limiting barrier of Ni in NiFe-MOF was significantly lower than that of Fe in NiFe-MOF and CeNiFe-MOF, suggesting that Ni atoms are the major active sites for the OER. As shown in Fig. 5c, the rate-determining step (RDS) on Ni sites of NiFe-MOF and CeNiFe-MOF is the conversion of OH\* to O\*. It was found that the energy barrier of RDS decreased from 2.15 to 1.82 eV after incorporating Ce into NiFe-MOF, implying that the introduction of Ce is beneficial to stimulate the OER

process.<sup>37,72</sup> Additionally, the calculations also manifested that Ce is highly efficient for the electrocatalytic OER but inactive for the HER (Fig. 5d and S35†). The above results demonstrated that Ce doping played a key role in modulating the electronic structure of reaction sites and optimizing the adsorption of intermediates, thus leading to superior HER and OER performance.

To further demonstrate the universality of this doping engineering for performance boost, other rare-earth elements such as Y and La were also introduced into NiFe-MOF to prepare the self-supporting YNiFe-MOF and LaNiFe-MOF electrodes. XRD measurements confirmed their successful preparation (Fig. S36†). As expected, YNiFe-MOF and LaNiFe-MOF were found to exhibit enhanced electrocatalytic properties for both the HER and OER in different electrolytes, including lower reaction overpotentials, smaller Tafel slopes, larger  $C_{dl}$  values, higher specific activity and faster charge transport (Fig. S37–S44†), which further indicated the important role of rare-earth doping in performance optimization.





- 49 Y. Yang, H. Q. Yao, Z. H. Yu, S. M. Islam, H. Y. He, M. W. Yuan, Y. H. Yue, K. Xu, W. C. Hao, G. B. Sun, H. F. Li, S. L. Ma, P. Zapol and M. G. Kanatzidis, *J. Am. Chem. Soc.*, 2019, **141**, 10417–10430.
- 50 Z. Q. Xue, X. Li, Q. L. Liu, M. K. Cai, K. Liu, M. Liu, Z. F. Ke, X. L. Liu and G. Q. Li, *Adv. Mater.*, 2019, **31**, 1900430.
- 51 X. X. Wu, T. Zhang, J. X. Wei, P. F. Feng, X. B. Yan and Y. Tang, *Nano Res.*, 2020, **13**, 2130–2135.
- 52 Y. Z. Liu, X. T. Li, Q. D. Sun, Z. L. Wang, W. H. Huang, X. Y. Guo, Z. X. Fan, R. Q. Ye, Y. Zhu, C. C. Chueh, C. L. Chen and Z. L. Zhu, *Small*, 2022, **18**, 2201076.
- 53 D. S. Raja, C. L. Huang, Y. A. Chen, Y. M. Choi and S. Y. Lu, *Appl. Catal., B*, 2020, **279**, 119375.
- 54 C. X. Zhang, Q. L. Qi, Y. J. Mei, J. Hu, M. Z. Sun, Y. J. Zhang, B. L. Huang, L. B. Zhang and S. H. Yang, *Adv. Mater.*, 2023, **35**, 2208904.
- 55 T. Yamashita and P. Hayes, *Appl. Surf. Sci.*, 2008, **254**, 2441–2449.
- 56 H. J. Xu, B. K. Wang, C. F. Shan, P. X. Xi, W. S. Liu and Y. Tang, *ACS Appl. Mater. Interfaces*, 2018, **10**, 6336–6345.
- 57 J. Yu, Y. Qian, Q. Wang, C. Su, H. Lee, L. Shang and T. Zhang, *EES Catal.*, 2023, **1**, 571–579.
- 58 M. Zhao, W. Li, J. Y. Li, W. H. Hu and C. M. Li, *Adv. Sci.*, 2020, **7**, 2001965.
- 59 S. L. Lyu, C. X. Guo, J. N. Wang, Z. J. Li, B. Yang, L. C. Lei, L. P. Wang, J. P. Xiao, T. Zhang and Y. Hou, *Nat. Commun.*, 2022, **13**, 6171.
- 60 K. Ge, S. J. Sun, Y. Zhao, K. Yang, S. Wang, Z. H. Zhang, J. Y. Cao, Y. F. Yang, Y. Zhang, M. W. Pan and L. Zhu, *Angew. Chem., Int. Ed.*, 2021, **60**, 12097–12102.
- 61 F. P. Cheng, X. Y. Peng, L. Z. Hu, B. Yang, Z. J. Li, C. L. Dong, E. L. Chen, L. C. Hsu, L. C. Lei, Q. Zheng, M. Qiu, L. M. Dai and Y. Hou, *Nat. Commun.*, 2022, **13**, 6486.
- 62 Y. M. Sun, Z. Q. Xue, Q. L. Liu, Y. L. Jia, Y. L. Li, K. Liu, Y. Y. Lin, M. Liu, G. Q. Li and C. Y. Su, *Nat. Commun.*, 2021, **12**, 1369.
- 63 Y. R. Wang, A. N. Wang, Z. Z. Xue, L. Wang, X. Y. Li and G. M. Wang, *J. Mater. Chem. A*, 2021, **9**, 22597–22602.
- 64 Y. S. Chen, J. K. Wang, Z. B. Yu, Y. P. Hou, R. H. Jiang, M. Wang, J. Huang, J. H. Chen, Y. Q. Zhang and H. X. Zhu, *Appl. Catal., B*, 2022, **307**, 121151.
- 65 J. Sun, Z. Zhang and X. Meng, *Appl. Catal., B*, 2023, **331**, 122703.
- 66 Y. Jiang, T.-Y. Chen, J.-L. Chen, Y. Liu, X. Yuan, J. Yan, Q. Sun, Z. Xu, D. Zhang, X. Wang, C. Meng, X. Guo, L. Ren, L. Liu and R. Y.-Y. Lin, *Adv. Mater.*, 2024, **36**, 2306910.
- 67 S. Zhang, Z. Huang, T. T. Isimjan, D. Cai and X. Yang, *Appl. Catal., B*, 2024, **343**, 123448.
- 68 L. Song, L. Guo, J. Mao, Z. Li, J. Zhu, J. Lai, J. Chi and L. Wang, *ACS Catal.*, 2024, **14**, 6981–6991.
- 69 Q. Hu, K. Gao, X. Wang, H. Zheng, J. Cao, L. Mi, Q. Huo, H. Yang, J. Liu and C. He, *Nat. Commun.*, 2022, **13**, 3958.
- 70 X. W. Chang, S. Li, L. Wang, L. Dai, Y. P. Wu, X. Q. Wu, Y. Tian, S. Zhang and D. S. Li, *Adv. Funct. Mater.*, 2024, **34**, 2313974.
- 71 J. Zhou, P. Li, X. Xia, Y. Zhao, Z. Hu, Y. Xie, L. Yang, Y. Liu, Y. Du, Q. Zhou, L. Yu and Y. Yu, *Appl. Catal., B*, 2024, **359**, 124461.
- 72 F. P. Cheng, Z. J. Li, L. Wang, B. Yang, J. G. Lu, L. C. Lei, T. Y. Ma and Y. Hou, *Mater. Horiz.*, 2021, **8**, 556–564.

